Subcritical Hopf bifurcation in the dynamics of a pressure relief valve

Fanni Kádár[†] and Gabor Stepan[†]
[†]*Department of Applied Mechanics , Budapest University of Technology and Economics, Budapest, Hungary*

Summary. The direct spring operated pressure relief valves are prone to harmful vibrations, which endanger the protected system under pressure. The studied mathematical model describes a system consisting of a vessel and of a pressure relief valve mounted on the vessel. The mathematical model with the state variables of valve lift, valve disk velocity and vessel pressure shows strong asymmetric nonlinearities. Our adapted numerical simulation is appropriate to produce bifurcation diagrams with the bifurcation parameter of the inlet flow rate, and also to draw the phase portrait. At the certain range of parameter combinations the equilibrium state loses the stability through subcritical Hopf bifurcation. In the case of dense parameter sweep in the phase space an unstable limit cycle appears between the trajectories. This unstable limit cycle can be calculated analytically by executing the Hopf bifurcation calculation. In comparison with the numerical unstable limit cycle, we studied the effect of the asymmetry of the nonlinearties on the analytically calculated unstable limit cycle. Global bifurcation diagram is constructed to trace the dynamical behaviour of the system 'outside' the unstable limit cycle, which includes impacts with the valve seat.

Introduction

The mathematical model of the direct spring operated pressure relief valve (see Fig. 1a) can be derived from the Newtonian equation of the valve disk and from the mass balance equation of the vessel [1]:

$$y_1' = y_2\,, \tag{1}$$
$$y_2' = -\kappa y_2 - (y_1 + \delta) + y_3\,, \tag{2}$$
$$y_3' = \beta\,(q - \sqrt{y_3}y_1)\,, \tag{3}$$

where the dimensionless coordinates $y_{1,2,3}$ represent the valve lift, the valve disk velocity and the overpressure in the vessel, respectively. The dimensionless parameters are the inlet flow rate q, the damping coefficient κ, the opening pressure δ, and stiffness β of the fluid, which are obtained from the physical parameters in Fig. 1a according to the following formulas:

$$q = \frac{Q_{\text{in}}}{\frac{Ap_0}{k} D\pi C_d \sqrt{\frac{2p_0}{\rho}}}\,, \quad \kappa = \frac{b}{m}\sqrt{\frac{m}{k}}\,, \quad \delta = \frac{kx_0}{Ap_0} = \frac{p_{\text{open}}}{p_0}\,, \quad \beta = \sqrt{\frac{m}{k}}\frac{E}{V}\frac{AD\pi}{k}\sqrt{\frac{2p_0}{\rho}}\,.$$

During operation, only the flow rate q can change, which is chosen as bifurcation parameter. The volume V of the vessel is inversely proportional to the β, and it has an essential influence on the stability of the equilibrium state and also on the type of stability loss. Figure 2a shows a stability diagram of the equilibrium in the plane of the parameters q and β. It can be seen that the system is stable for small and large β values. We study the loss of stability at $\beta = 10$, which belongs to the small vessel volume. For this data the bifurcation diagram is shown in Figure 2b. The analytically calculated and numerically checked critical flow rate value at the Hopf bifurcation is $q_{\text{cr}} = 5.930$.

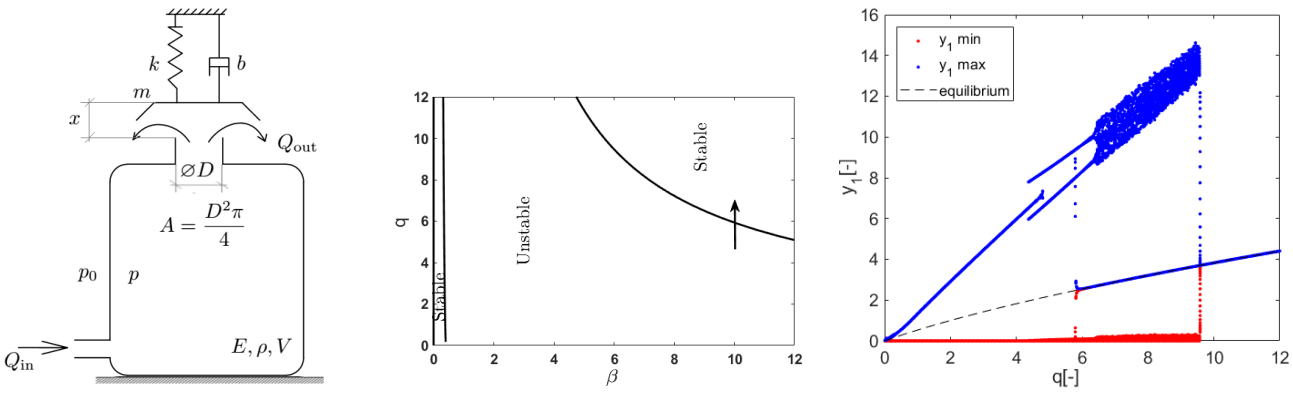

(a) Mechanical model (b) Stability chart for $\kappa = 0.7\,, \delta = 3$ (c) Bifurcation diagram for $\beta = 10$

Figure 1: Modelling, stability and bifurcations of the pressure relief valve

Nonlinear analysis

The 3^{rd} degree approximation of the system (1-3) around the equilibrium y_{10}, y_{20}, y_{30} has the form:

$$\begin{bmatrix}\xi_1'\\ \xi_2'\\ \xi_3'\end{bmatrix} = \begin{bmatrix}0 & 1 & 0\\ -1 & -\kappa & 1\\ -\beta\sqrt{y_{30}} & 0 & -\beta\frac{y_{10}}{2\sqrt{y_{30}}},\end{bmatrix}\begin{bmatrix}\xi_1\\ \xi_2\\ \xi_3\end{bmatrix} + \begin{bmatrix}0\\ 0\\ \beta\left(-\frac{1}{2\sqrt{y_{30}}}\xi_1\xi_3 + \frac{y_{10}}{8\sqrt{y_{30}^3}}\xi_3^2 + \frac{1}{8\sqrt{y_{30}^3}}\xi_1\xi_3^2 - \frac{y_{10}}{16\sqrt{y_{30}^5}}\xi_3^3\right)\end{bmatrix} \tag{4}$$

At the bifurcation point, the linear part has the eigenvalues $\lambda_{1,2} = \pm i\omega, \lambda_3 := \lambda \in \Re^-$. Since the nonlinearity is strongly asymmetric, there are 2^{nd} degree terms in Eq. (4). Consequently, the system has to be reduced to the centre manifold that is approximated by 2^{nd} degree terms, too. The centre manifold can be calculated in the eigenbasis of coordinates (u_1, u_2, u_3), and it is tangent to the plane spanned by the complex conjugate eigenvectors. The lengthy algebraic calculation involves also the Near Identity transformation:

$$\begin{bmatrix}u_1\\ u_2\end{bmatrix} = \mathbf{I}\begin{bmatrix}v_1\\ v_2\end{bmatrix} + \begin{bmatrix}\sum_{j+k=\{2,3\}}\varphi_{jk}(\mu)v_1^j v_2^k\\ \sum_{j+k=\{2,3\}}\psi_{jk}(\mu)v_1^j v_2^k\end{bmatrix}, \tag{5}$$

which leads to the 3^{rd} order normal form for (v_1, v_2). This way, we obtain the Poincare-Lyapunov constant $\Delta = 0.028 > 0$, which refers to subcritical Hopf bifurcation. The emerging unstable limit cycle has the amplitude:

$$r = \sqrt{-\frac{\text{Re}\lambda_{1,2}'\big|_{q=q_{\text{cr}}}}{\Delta}(q - q_{\text{cr}})}, \tag{6}$$

where the root tendency $\text{Re}\lambda_{1,2}' = -0.046 < 0$ can be calculated from the characteristic equation by implicit derivation with respect to the bifurcation parameter q. Through a polar coordinate transformation $v_1 = r\cos(\omega\tau), v_2 = r\sin(\omega\tau)$. Transforming back only the linear part of Eq. (5) to the original phase space makes the calculation easier, and has a sufficient result for symmetric systems [2], but Fig. 2b shows with dashed red line how this treatment effects the location of the limit cycle for this strongly asymmetric case. The limit cycle can fit better to the numeric unstable limit cycle when the 2^{nd} degree terms are transformed back, too. After the polar coordinate transformation, the second degree terms result in constant and $\sin(2\omega\tau), \cos(2\omega\tau)$ terms multiplied by r^2. If the linear system is shifted with this constant only, then the unstable limit cycle is shown by red continuous line in Fig. 2b. The trace of the unstable limit cycle fits best by transforming back also the 2^{nd} degree terms, which is represented with red dots in Fig. 2b.

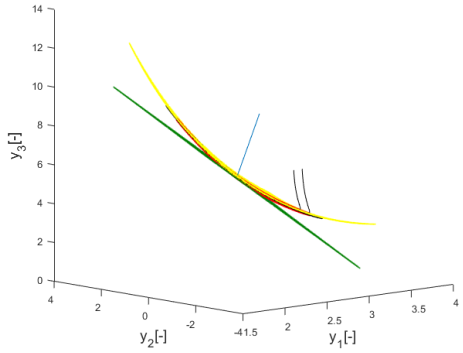

(a) Centre manifold (yellow), tangent plane (green), two numerical trajectories (black), analytical limit cycle (red)

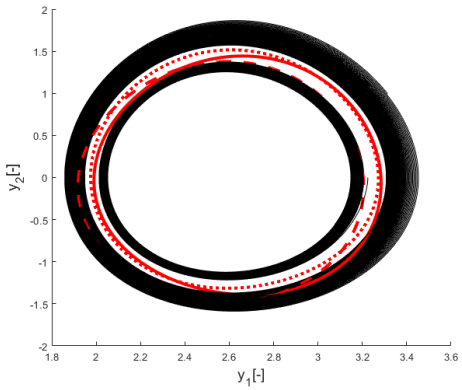

(b) A stable and an unstable numerical trajectories (black) embracing the unstable limit cycle (white) and analytical limit cycles with 3 different approximations (red)

Figure 2: Numerical and analytical results presented in the phase space of pressure relief valve

The global dynamics of the system 'outside' the unstable limit cycle is determined by the impacts of the valve disk and the seat. This is characterized by the numerical bifurcation diagram in Fig. 1c, which fits perfectly to the analytically predicted unstable limit cycle.

References

[1] Licskó G., Champneys A., Hős Cs. (2009) Nonlinear Analysis of a Single Stage Pressure Relief Valve. *IAENG International Journal of Applied Mathematics* **39**:4.

[2] Stepan G. (1991) Chaotic Motion of Wheels. *Vehicle System Dynamics* **20(6)** pp. 341-351.